Journal of Sound and Vibration 379 (2016) 150–165

Contents lists available at ScienceDirect

Journal of Sound and Vibration

journal homepage: www.elsevier.com/locate/jsvi

An analytical approach for detecting isolated periodic solution branches in weakly nonlinear structures

T.L. Hill [a,*], S.A. Neild [a], A. Cammarano [b]

[a] Department of Mechanical Engineering, Queen's Building, University of Bristol, Bristol BS8 1TR, UK
[b] School of Engineering, University of Glasgow, Glasgow G12 8QQ, UK

ARTICLE INFO

Article history:
Received 10 January 2016
Received in revised form
5 May 2016
Accepted 17 May 2016
Handling Editor: L.N. Virgin
Available online 10 June 2016

Keywords:
Isolas
Detached resonance curves
Second-order normal form technique
Backbone curves
Isolated backbone curves
Energy transfer analysis

ABSTRACT

This paper considers isolated responses in nonlinear systems; both in terms of isolas in the forced responses, and isolated backbone curves (i.e. the unforced, undamped responses). As isolated responses are disconnected from other response branches, reliably predicting their existence poses a significant challenge. Firstly, it is shown that breaking the symmetry of a two-mass nonlinear oscillator can lead to the breaking of a bifurcation on the backbone curves, generating an isolated backbone. It is then shown how an energy-based, analytical method may be used to compute the points at which the forced responses cross the backbone curves at resonance, and how this may be used as a tool for finding isolas in the forced responses. This is firstly demonstrated for a symmetric system, where an isola envelops the *secondary* backbone curves, which emerge from a bifurcation. Next, an asymmetric configuration of the system is considered and it is shown how isolas may envelop a primary backbone curve, i.e. one that is connected directly to the zero-amplitude solution, as well as the isolated backbone curve. This is achieved by using the energy-based method to determine the relationship between the external forcing amplitude and the positions of the crossing points of the forced response. Along with predicting the existence of the isolas, this technique also reveals the nature of the responses, thus simplifying the process of finding isolas using numerical continuation.

1. Introduction

Due to the complexity of the dynamic responses of nonlinear structures, their computation can be quite challenging. This is, in part, the result of features such as bifurcations, internal resonances, and multiple solutions, which are primarily observed in the presence of nonlinearity. In many engineering applications the steady-state responses are of primary interest and, when a structure exhibits nonlinear characteristics, the approaches for computing these responses consist of analytical and numerical techniques. Analytical techniques include the harmonic balance method, multiple scale analysis, and the method of normal forms [1–3]. Software packages for the numerical computation of such responses include AUTO-07p [4], Computational Continuation Core (COCO) [5], and NNMcont (based upon the theory of nonlinear normal modes) [6].

One advantage of using analytical methods to find the periodic responses of nonlinear systems is that, in some instances, approximate closed-form solutions may be obtained. As well as allowing solutions to be found efficiently, this also allows them to be found directly, without the need for initial solutions. However, in many instances, closed-form solutions cannot

* Corresponding author.
E-mail address: tom.hill@bristol.ac.uk (T.L. Hill).

http://dx.doi.org/10.1016/j.jsv.2016.05.030
0022-460X/

be obtained, such as when the system is large or the nonlinearity is complex. In such instances, numerical approaches may be adopted to solve the approximate analytical expressions, as has been demonstrated with the numerical implementation of the harmonic balance method [7,8]. Alternatively, purely numerical approaches may be employed; however, these approaches typically rely upon continuation, which requires an initial solution and can only be used to find new solutions that form part of a continuous branch. Whilst these approaches are advanced and highly efficient, they are not readily suited for finding *isolas* – i.e. solutions that are detached from the main, or *primary*, response branches – directly unless a solution on, or an approximate solution in the vicinity of, the isola is known.

One numerical approach that may be used to find isolas is the continuation of fold bifurcations, as discussed in [9]; however, some isolas may only be reached using a specific choice of continuation parameters, and thus require a good understanding of the behaviour of the system. Another numerical approach is global analysis [10], which involves simulating the system for numerous initial conditions, and finding the resulting steady-state, or *near-steady-state*, responses. An isola will be revealed if initial conditions are selected that are within the basin of attraction of that isola. This approach is rigorous, provided a sufficiently large number of initial conditions are simulated; however this is often computationally expensive, especially for systems with large numbers of degrees-of-freedom.

As isolas are detached from the primary response branches, finding them typically relies upon a priori knowledge of their existence; however there is currently no rigorous, and efficient, method for determining the existence of isolas. The significance of this was demonstrated in a paper by Alexander and Schilder [11], who discovered an isola in the dynamic response of a nonlinear tuned mass damper. Despite extensive investigation prior to this, the existence of this isola was unknown, and hence its dynamic behaviour had not been described.

This paper introduces a method for finding isolas in nonlinear dynamic systems. This method uses the backbone curves, i.e. the loci of unforced, undamped responses, alongside an energy-based method. The requirement that the analytical expressions for the backbone curves may be solved does limit this approach; however it is shown here that the backbone curves represent a computationally simpler problem than the forced responses. As such, finding *isolated* backbone curves, i.e. backbone curves that are not connected to primary backbone curves, is typically simpler than finding isolas in the forced responses.

In order to demonstrate the approach for finding isolas, a conceptually simple, two-mass oscillator is introduced in Section 2 and is considered throughout this paper. This oscillator may be used to represent a number of typical engineering systems, such as tuned-mass dampers, and can also be used to represent the dynamics of continuous structures, such as cables [12]. To compute the backbone curves of the example system, the second-order normal form technique is employed. This analytical technique was first introduced in [13] and its application to backbone curves was demonstrated in [14].

When the two-mass oscillator has a symmetric configuration, a bifurcation exists in the backbone curves, as shown in [14]. This is briefly demonstrated in Section 2.2 before, in Section 2.3, a number of asymmetric configurations are considered. It is shown that the breaking of the symmetry leads to an isolated backbone curve, via a breaking of the bifurcation on the backbone curve, forming an *imperfect* bifurcation [15]. As closed-form solutions are obtained using the analytical technique, finding these isolated backbone curves does not present any additional computational challenge. Next, in Section 3, the energy-based method for relating backbone curves to resonant forced responses is applied to the oscillator. This is based upon the procedure that was first introduced in [16], and further developed in [17], and is used to estimate the points at which the backbone curves are crossed by the forced responses at resonance, known as the resonant crossing points.

The forced responses of the symmetric configuration of the system are investigated in Section 4, where it is shown that isolas may envelop the bifurcated backbone curves. The existence of these isolas is predicted using the backbone curves and resonant crossing points. In Section 5 the asymmetric configuration is considered for a number of different forcing cases, and it is firstly demonstrated that isolas that envelop the primary backbone curves may exist. Similar isolas have previously been demonstrated in [9] and have been found experimentally in [18,19]. It is then shown that an isola may also exist on the isolated backbone curve – a feature that requires a priori knowledge of both the isolated backbone curve and the locations of the resonant crossing points on that backbone curve, both of which are provided by the technique presented here. A final forcing case, where external forcing is applied to only one mass, is then considered and it is shown that an isola with resonant crossing points on the isolated backbone curve may also exist. Finally, conclusions are drawn in Section 6.

2. Isolated backbone curves

2.1. The backbone curves of an example system

In this paper, the 2-DOF oscillator, represented by the schematic diagram in Fig. 1, is considered and its backbone curves, i.e. the loci of responses of the equivalent conservative system, are computed. This oscillator consists of two equal masses, both of mass m, with displacements x_1 and x_2 for the first and second masses respectively. These masses are both grounded by identical linear springs, with stiffness k_1, and are coupled via an additional linear spring, with stiffness k_2. As a result, it can be seen that the underlying linear structure of this system is symmetric. The oscillator also contains three cubic nonlinear springs with the force–displacement relationships $F=\alpha_i(\Delta x)^3$, where α_i is a nonlinear constant and Δx is the deflection of the spring. Two of these nonlinear springs, with constants α_1 and α_3, ground the masses, and one nonlinear spring, with constant α_2, couples the masses. Two identical linear, viscous dampers, with damping constant c_1, ground the

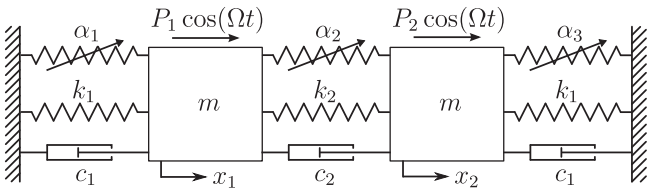

Fig. 1. A schematic of a two-mass oscillator with three nonlinear springs.

masses; and an additional damper, with constant c_2, couples the masses. Additionally, the first and second masses are forced sinusoidally at amplitudes P_1 and P_2 respectively, and both at frequency Ω.

A symmetric configuration of this system, i.e. where $\alpha_1 = \alpha_3$, is considered in Section 2.2 where it is shown that the backbone curves may exhibit bifurcations, leading to additional backbone curves. Note that a similar case has previously been considered in [14]. We now outline how the second-order normal form technique may be used to find analytical expressions describing these responses. This technique has previously been discussed in detail in [13,20], and has been used to find the backbone curves of a similar system in [21]. As such, only a brief outline of the derivation of the backbone curve expressions is presented here.

The equations of motion for a general oscillator may be written as

$$\mathbf{M}\ddot{\mathbf{x}} + \mathbf{C}\dot{\mathbf{x}} + \mathbf{K}\mathbf{x} + \mathbf{N}_x(\mathbf{x}, \dot{\mathbf{x}}, t) = \mathbf{P}\cos(\Omega t), \tag{1}$$

where $\mathbf{M}$, $\mathbf{C}$ and $\mathbf{K}$ are the mass, damping and stiffness matrices respectively, and $\mathbf{x}$, $\mathbf{N}_x$ and $\mathbf{P}$ are vectors of displacements, nonlinear terms and forcing amplitudes respectively. Note that $\mathbf{N}_x$ may incorporate nonlinear stiffness, damping and forcing terms; however only the stiffness terms affect the backbone curves. For the system considered here, these are written as

$$\begin{gathered}\mathbf{M} = \begin{bmatrix} m & 0 \\ 0 & m \end{bmatrix}, \quad \mathbf{C} = \begin{bmatrix} c_1+c_2 & -c_2 \\ -c_2 & c_1+c_2 \end{bmatrix}, \quad \mathbf{K} = \begin{bmatrix} k_1+k_2 & -k_2 \\ -k_2 & k_1+k_2 \end{bmatrix}, \\ \mathbf{N}_x = \begin{pmatrix} \alpha_1 x_1^3 + \alpha_2 (x_1 - x_2)^3 \\ \alpha_3 x_2^3 + \alpha_2 (x_2 - x_1)^3 \end{pmatrix}, \quad \mathbf{P} = \begin{pmatrix} P_1 \\ P_2 \end{pmatrix}, \quad \mathbf{x} = \begin{pmatrix} x_1 \\ x_2 \end{pmatrix}.\end{gathered} \tag{2}$$

To compute the backbone curves of a system, the forcing and damping terms are typically set to zero at this stage, simplifying the equations of motion. However the energy-based analysis, considered later in this paper, requires that the nonconservative terms are retained for now.

The first step of the second-order normal form technique, the linear modal transform, is applied to Eq. (1) in order to decouple the linear components of the system. This is achieved using the substitution $\mathbf{x} = \mathbf{\Phi}\mathbf{q}$, where $\mathbf{\Phi}$ is a linear modeshape matrix and $\mathbf{q}$ is a vector of linear modal displacements. This transform results in the modal equations of motion, written as

$$\ddot{\mathbf{q}} + \mathbf{\Lambda}\mathbf{q} + \mathbf{N}_q(\mathbf{q}, \dot{\mathbf{q}}) = \mathbf{P}_q \cos(\Omega t), \tag{3}$$

where $\mathbf{\Lambda}$ is a diagonal matrix containing the squares of the linear natural frequencies, $\mathbf{N}_q$ is a vector of nonlinear and damping terms, and $\mathbf{P}_q$ is a vector of modal forcing amplitudes. From Eqs. (1) and (2), these are written as

$$\begin{gathered}\mathbf{\Lambda} = \begin{bmatrix} \omega_{n1}^2 & 0 \\ 0 & \omega_{n2}^2 \end{bmatrix} = \frac{1}{m}\begin{bmatrix} k_1 & 0 \\ 0 & k_1+2k_2 \end{bmatrix}, \quad \mathbf{\Phi} = \begin{bmatrix} 1 & 1 \\ 1 & -1 \end{bmatrix}, \\ \mathbf{P}_q = \begin{pmatrix} P_{q1} \\ P_{q2} \end{pmatrix} = \frac{1}{2m}\begin{pmatrix} P_1+P_2 \\ P_1-P_2 \end{pmatrix}, \quad \mathbf{q} = \begin{pmatrix} q_1 \\ q_2 \end{pmatrix}, \\ \mathbf{N}_q = \begin{pmatrix} 2\zeta_1\omega_{n1}\dot{q}_1 \\ 2\zeta_2\omega_{n2}\dot{q}_2 \end{pmatrix} + \frac{1}{2m}\begin{pmatrix} \alpha_1(q_1+q_2)^3 + \alpha_3(q_1-q_2)^3 \\ \alpha_1(q_1+q_2)^3 + \alpha_3(q_2-q_1)^3 + 16\alpha_2 q_2^3 \end{pmatrix},\end{gathered} \tag{4}$$

where $2\zeta_1\omega_{n1} = c_1/m$ and $2\zeta_2\omega_{n2} = (c_1+2c_2)/m$. Here it is assumed that the linear modal damping ratios are equal, i.e. $\zeta_1 = \zeta_2 = \zeta$, which is achieved when $2c_2 = (\omega_{n2}/\omega_{n1} - 1)c_1$. Note that, as the modeshapes of the equivalent linear system have been used, cross-coupling via the nonlinear terms remains in the modal equations of motion – here, the term *modal* is used to denote the underlying linear modes of the system. Additionally, note that in the examples considered here, the linear natural frequencies are close, i.e. $\omega_{n1} \approx \omega_{n2}$; hence it may be assumed that the fundamental components of these linear modes will respond at the same frequency. When $\omega_{n1} \not\approx \omega_{n2}$, the system may exhibit responses where the fundamental components of the modes have different, but commensurate, frequencies – see, for example, [18].

The next step in the second-order normal form technique is the forcing transform, which seeks to remove any non-resonant external forcing terms from the equations of motion. Here, however, it is assumed that all external forcing is resonant, i.e. it is assumed that the fundamental response of both modes is at the forcing frequency, Ω; as such, this is a unity transform and so is not applied here. For examples of the application of the forcing transform in the presence of non-

resonant forcing, see [13,22]. The following step, the nonlinear near-identity transform, involves the substitution $\mathbf{q}=\mathbf{u}+\mathbf{h}$ where $\mathbf{u}$ and $\mathbf{h}$ are vectors describing the fundamental and harmonic components of $\mathbf{q}$ respectively.

The second-order normal form technique relies on the assumption that the nonlinear and damping terms are small, in comparison to the undamped linear terms, and that the harmonics are also small, in comparison to the fundamental components. Therefore, it may be assumed that the contribution of the harmonic components to the nonlinear and damping terms is negligible, and hence the approximation $\mathbf{q}=\mathbf{u}$ may be substituted into the vector of modal damping and nonlinear terms, $\mathbf{N}_q(\mathbf{q},\dot{\mathbf{q}})$. Additionally, it is assumed that the fundamental components of the response are sinusoidal, and hence the ith element of $\mathbf{u}$, i.e. the fundamental component of the ith mode, may be written as

$$u_i = U_i\cos\left(\omega_{ri}t-\phi_i\right)=u_{pi}+u_{mi}=\frac{U_i}{2}\mathrm{e}^{+\mathrm{j}(\omega_{ri}t-\phi_i)}+\frac{U_i}{2}\mathrm{e}^{-\mathrm{j}(\omega_{ri}t-\phi_i)}, \tag{5}$$

where U_i, ω_{ri} and ϕ_i represent the amplitude, response frequency and phase of u_i respectively. Note that ω_{ri} and ω_{ni} are distinct, and represent the ith response frequency and linear natural frequency respectively. Additionally, note that the subscripts p and m denote the positive and negative (i.e. *plus* and *minus*) signs of the exponents respectively.

This transform results in the resonant equation of motion, written as

$$\ddot{\mathbf{u}}+\mathbf{\Lambda}\mathbf{u}+\mathbf{N}_u(\mathbf{u},\dot{\mathbf{u}})=\mathbf{P}_u\cos\left(\Omega t\right), \tag{6}$$

where $\mathbf{N}_u$ is a vector of resonant nonlinear and damping terms. As it is assumed that the fundamental components of the modes, $\mathbf{u}$, respond at the forcing frequency, i.e. $\omega_{r1}=\omega_{r2}=\Omega$, then all terms in $\mathbf{N}_u$ must resonate at frequency Ω. It therefore follows that $\mathbf{P}_u=\mathbf{P}_q$. Note that expressions for the harmonic components, in terms of $\mathbf{u}$, may also be developed; however, for the cases considered here, the harmonics are neglected. For details of how the harmonics may be computed, see [23,24].

After making the substitution $\mathbf{q}=\mathbf{u}$ and $\dot{\mathbf{q}}=\dot{\mathbf{u}}$ into $\mathbf{N}_q(\mathbf{q},\dot{\mathbf{q}})$, the resonant components may be identified and used to populate the vector of resonant nonlinear terms, written as

$$\mathbf{N}_u=2\zeta\begin{pmatrix}\omega_{n1}\dot{u}_1\\ \omega_{n2}\dot{u}_2\end{pmatrix}+3\begin{pmatrix}\alpha_p\left[\left(u_{p1}u_{m1}+2u_{p2}u_{m2}\right)u_1+u_{p1}u_{m2}^2+u_{m1}u_{p2}^2\right]+\alpha_m\left[\left(2u_{p1}u_{m1}+u_{p2}u_{m2}\right)u_2+u_{p1}^2u_{m2}+u_{m1}^2u_{p2}\right]\\ \alpha_m\left[\left(u_{p1}u_{m1}+2u_{p2}u_{m2}\right)u_1+u_{p1}u_{m2}^2+u_{m1}u_{p2}^2\right]+\alpha_p\left[\left(2u_{p1}u_{m1}+u_{p2}u_{m2}\right)u_2+u_{p1}^2u_{m2}+u_{m1}^2u_{p2}\right]+8\frac{\alpha_2}{m}u_{p2}u_{m2}u_2\end{pmatrix}, \tag{7}$$

where

$$\alpha_p=\frac{\alpha_1+\alpha_3}{2m},\quad \alpha_m=\frac{\alpha_1-\alpha_3}{2m}. \tag{8}$$

Further details of this step, applied to a general nonlinear system, may be found in [13,20], and the application to a similar system to that considered here may be found in [21].

As it is known that all terms in the ith element of $\mathbf{N}_u$ respond at the forcing frequency, Ω, it may be written in terms of the time-independent components N_{ui}^+ and N_{ui}^-, such that

$$N_{ui}=N_{ui}^+\mathrm{e}^{+\mathrm{j}\Omega t}+N_{ui}^-\mathrm{e}^{-\mathrm{j}\Omega t}, \tag{9}$$

where N_{ui}^+ and N_{ui}^- are complex conjugates. Substituting this, along with the assumed solution for u_i, from Eq. (5), into the ith resonant equation of motion, from Eq. (6), leads to

$$\left[\left(\omega_{ni}^2-\Omega^2\right)\frac{U_i}{2}\mathrm{e}^{-\mathrm{j}\phi_i}+N_{ui}^+-\frac{P_{qi}}{2}\right]\mathrm{e}^{+\mathrm{j}\Omega t}+\left[\left(\omega_{ni}^2-\Omega^2\right)\frac{U_i}{2}\mathrm{e}^{+\mathrm{j}\phi_i}+N_{ui}^--\frac{P_{qi}}{2}\right]\mathrm{e}^{-\mathrm{j}\Omega t}=0, \tag{10}$$

where it has been recalled that $\mathbf{P}_u=\mathbf{P}_q$, and where the contents of the two square brackets are complex conjugates. As such, the first of these brackets may be equated to zero, to give a time-independent expression written as

$$\left(\omega_{ni}^2-\Omega^2\right)U_i+2N_{ui}^+\mathrm{e}^{+\mathrm{j}\phi_i}=P_{qi}\mathrm{e}^{+\mathrm{j}\phi_i}. \tag{11}$$

These expressions may be solved, for $i=1,2$, to find the forced response branches; however this can prove challenging, especially for larger and more complex systems. Instead, the backbone curves may be computed by setting the forcing and damping terms to zero. Hence, finding N_{u1}^+ and N_{u2}^+ from Eq. (7), and substituting these into Eq. (11) gives

$$\left(\omega_{n1}^2-\omega^2\right)U_1+\frac{3}{4}\left\{\alpha_p\left[U_1^3+U_1U_2^2\left(2+\mathrm{e}^{+\mathrm{j}2\phi_d}\right)\right]+\alpha_m\left[U_2^3+U_1^2U_2\left(2+\mathrm{e}^{-\mathrm{j}2\phi_d}\right)\right]\mathrm{e}^{+\mathrm{j}\phi_d}\right\}=0, \tag{12a}$$

$$\left(\omega_{n2}^2-\omega^2\right)U_2+\frac{3}{4}\left\{\alpha_p\left[U_2^3+U_1^2U_2\left(2+\mathrm{e}^{-\mathrm{j}2\phi_d}\right)\right]+\alpha_m\left[U_1^3+U_1U_2^2\left(2+\mathrm{e}^{+\mathrm{j}2\phi_d}\right)\right]\mathrm{e}^{-\mathrm{j}\phi_d}+8\frac{\alpha_2}{m}U_2^3\right\}=0, \tag{12b}$$

where $\phi_d=\phi_1-\phi_2$ and where the forcing and damping have been set to zero. Note that, as the backbone curves are

unforced, ω has been used in place of Ω, to represent the *common* response frequency of the two modes. These expressions may now be solved in order to find the backbone curves of this system.

2.2. Backbone curves of the symmetric configuration

We now consider a symmetric configuration of the 2-DOF oscillator, where $\alpha_1 = \alpha_3$ and hence, from Eq. (8), $\alpha_p = \alpha_1/m$ and $\alpha_m = 0$. Using this, Eqs. (12) may be written as

$$\left\{\omega_{n1}^2 - \omega^2 + \frac{3\alpha_1}{4m}\left[U_1^2 + U_2^2\left(2 + e^{+j2\phi_d}\right)\right]\right\}U_1 = 0, \tag{13a}$$

$$\left\{\omega_{n2}^2 - \omega^2 + \frac{3\alpha_1}{4m}\left[\gamma U_2^2 + U_1^2\left(2 + e^{-j2\phi_d}\right)\right]\right\}U_2 = 0, \tag{13b}$$

where $\gamma = 1 + 8\alpha_2/\alpha_1$.

The case where $U_1 = U_2 = 0$ is a trivial solution to Eqs. (13), corresponding to no motion. In addition to this, the modes may exist independently, resulting in two different backbone curves. The first of these backbone curves is denoted S_1, and contains only the first mode, i.e. $U_1 \neq 0$ and $U_2 = 0$. The second backbone curve, denoted S_2, is composed of only the second mode, i.e. $U_2 \neq 0$ and $U_1 = 0$. From Eqs. (13), these are described by the frequency–amplitude relationships

$$S_1: \quad U_2 = 0, \quad \omega^2 = \omega_{n1}^2 + \frac{3\alpha_1}{4m}U_1^2, \tag{14a}$$

$$S_2: \quad U_1 = 0, \quad \omega^2 = \omega_{n2}^2 + \frac{3\alpha_1\gamma}{4m}U_2^2. \tag{14b}$$

The case where $U_1 \neq 0$ and $U_2 \neq 0$ corresponds to a further set of solutions. This case leads to complex terms in Eqs. (13), and the imaginary components of these terms may both be written as

$$\sin\left(2\left[\phi_1 - \phi_2\right]\right) = 0, \tag{15}$$

where it has been recalled that $\phi_d = \phi_1 - \phi_2$. Eq. (15) may be satisfied by $\phi_1 - \phi_2 = 0, \frac{\pi}{2}, \pi, \ldots$, and hence the variable p may be defined, where

$$p = \cos\left(2\left[\phi_1 - \phi_2\right]\right) = \begin{cases} +1 & \text{when } \phi_1 - \phi_2 = 0, \pi, \ldots, \\ -1 & \text{when } \phi_1 - \phi_2 = \dfrac{\pi}{2}, \dfrac{3\pi}{2}, \ldots. \end{cases} \tag{16}$$

Substituting Eq. (16), into the real parts of Eqs. (13) gives

$$\omega^2 = \omega_{n1}^2 + \frac{3\alpha_1}{4m}\left[U_1^2 + U_2^2(2+p)\right], \tag{17a}$$

$$\omega^2 = \omega_{n2}^2 + \frac{3\alpha_1}{4m}\left[\gamma U_2^2 + U_1^2(2+p)\right]. \tag{17b}$$

In [12] it has been shown that the case where $p = -1$ may only lead to valid solutions when $\alpha_2 < 0$, i.e. the nonlinear spring that couples the masses exhibits softening behaviour. It is demonstrated that such solutions exhibit *out-of-unison resonance*, where the phase between the modes is $\pm 90^\circ$, as indicated by Eq. (16). Here, however, it is assumed that all springs are hardening, and hence only the $p = +1$ case is considered, which, from Eqs. (17), leads to the expressions

$$U_1^2 = \left(1 - \frac{4\alpha_2}{\alpha_1}\right)U_2^2 - \frac{2m}{3\alpha_1}\left(\omega_{n2}^2 - \omega_{n1}^2\right), \tag{18a}$$

$$\omega^2 = \frac{3\omega_{n1}^2 - \omega_{n2}^2}{2} + \frac{3(\alpha_1 - \alpha_2)}{m}U_2^2, \tag{18b}$$

describing the amplitude and frequency relationships of an additional set of backbone curves. From Eq. (16) it can be seen that the fundamental components of the two modes may be in-phase, i.e. $\phi_1 - \phi_2 = 0$, or in anti-phase, i.e. $\phi_1 - \phi_2 = \pi$. Therefore Eqs. (18) describe two backbone curves $S_{1,2}^+$ and $S_{1,2}^-$ (denoted $S_{1,2}^\pm$ when referring to both) which have the phase relationships

$$S_{1,2}^+: \quad \phi_1 - \phi_2 = 0, \tag{19a}$$

$$S_{1,2}^-: \quad \phi_1 - \phi_2 = \pi. \tag{19b}$$

Note that the subscripts of the backbone curve labels (S_1, S_2, $S_{1,2}^+$ and $S_{1,2}^-$) denote the modes that are present, whilst the superscripts denote the phase between the modes, where applicable. Due to the constant phase relationship between the modes, fewer variables are required in the computation of the backbone curves. This is in comparison to the computation of the forced responses, where the phase of each mode, with respect to the external forcing, must also be computed. This is

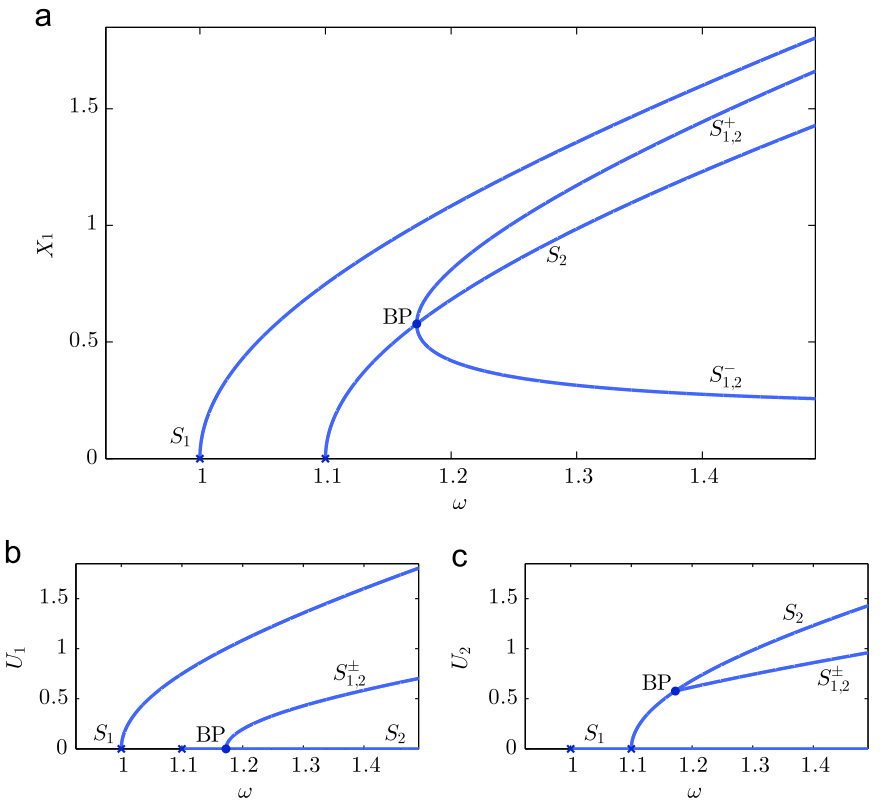

Fig. 2. The backbone curves of a symmetric, 2-DOF oscillator, where the single- and mixed-mode backbone curves, S_1, S_2 and $S^{\pm}_{1,2}$, are represented by solid-blue lines. Dark-blue crosses mark the linear natural frequencies, ω_{n1} and ω_{n2}, and a dark-blue dot, labelled "BP", represents a bifurcation from S_2 onto $S^{\pm}_{1,2}$. The three panels are in the projection of the common response frequency, ω, against: (a) the amplitude of displacement of the first mass, X_1; (b) the fundamental response amplitude of the first mode, U_1; (c) the fundamental response amplitude of the second mode, U_2. The parameter values for this system are provided in Table 1. (For interpretation of the references to colour in this figure caption, the reader is referred to the web version of this paper.)

Table 1
The parameter values for the 2-DOF oscillator, used for all examples given in this paper. Note that, in Fig. 3, a number of different values for α_3 are compared. Additionally, various different forcing amplitudes are employed throughout, and hence are not listed here.

Parameter	m	ω_{n1}	ω_{n2}	ζ	α_1	α_2	α_3
Symmetric configuration Asymmetric configuration 0.4→0.6	1	1	1.1	0.5%	0.5	0.02	0.5

particularly important for larger systems, where numerical approaches become necessary to when computing the forced responses.

In order to find the physical displacements, x_1 and x_2, the linear modal transform is used, which, from Eqs. (4), leads to $x_1 = q_1 + q_2$ and $x_2 = q_1 - q_2$. Therefore, neglecting harmonics such that $q_i = u_i$, the physical displacement amplitudes are written: $X_1 = U_1 + U_2$ and $X_2 = |U_1 - U_2|$ when the modes are in-phase; and $X_1 = |U_1 - U_2|$ and $X_2 = U_1 + U_2$ when the modes are in anti-phase.

Fig. 2 shows the backbone curves of the system, for the parameters given in Table 1, and calculated using Eqs. (14) and (18). It can be seen that the single mode backbone curves, S_1 and S_2, emerge from the trivial, zero-amplitude solution, and that the mixed-mode backbone curves, $S^{\pm}_{1,2}$, emerge from a bifurcation on S_2. This is discussed in detail in [14], where it is shown that a bifurcation is only present when $\alpha_1 > 4\alpha_2$, a condition which is satisfied by the system considered here.

As previously discussed, the computation of the physical displacement amplitudes is dependent on the phase difference between the modes. As such, in Fig. 2(a), which shows the displacement amplitude of the first mass, X_1, it can be seen that the backbone curves $S^{+}_{1,2}$ and $S^{-}_{1,2}$ are distinct. However, in Fig. 2(b) and (c), which shows the amplitudes U_1 and U_2 respectively, these backbone curves are superposed, as the modal projections are independent of phase. Furthermore, if Fig. 2(a) were shown in the projection of ω against X_2, this plot would look identical, except that $S^{+}_{1,2}$ and $S^{-}_{1,2}$ would be interchanged.

Here the backbone curves labelled S_1 and S_2 are defined as *primary* backbone curves, as they emerge from a zero-amplitude, trivial solution at the two linear natural frequencies. The backbone curves $S_{1,2}^{+}$ are known as *secondary* backbone curves as they bifurcate from primary backbone curves. Whilst secondary backbone curves do not emerge from the trivial solution, they are connected to backbone curves which do, and hence can be traced back to the trivial solution. As such, provided the primary backbone curves may be computed and the bifurcations are detected, these secondary branches may be found using continuation-based methods.

2.3. Backbone curves of an asymmetric configuration

The asymmetric configuration of the system, where $\alpha_1 \neq \alpha_3$, is now considered. Returning to the resonant equations of motion, Eqs. (12), the imaginary parts are now written as

$$\left[\alpha_p U_1 U_2 \sin(2\phi_d) + \alpha_m\left(U_2^2 + U_1^2\right)\sin(\phi_d)\right]U_2 = 0, \tag{20a}$$

$$\left[\alpha_p U_1 U_2 \sin(2\phi_d) + \alpha_m\left(U_1^2 + U_2^2\right)\sin(\phi_d)\right]U_1 = 0, \tag{20b}$$

and the real parts of Eqs. (12) are given by

$$(\omega_{n1}^2-\omega^2)U_1 + \frac{3}{4}\left\{\alpha_p\left[U_1^3 + U_1U_2^2(1+2\cos^2(\phi_d))\right] + \alpha_m\left[U_2^3 + 3U_1^2U_2\right]\cos(\phi_d)\right\} = 0, \tag{21a}$$

$$(\omega_{n2}^2-\omega^2)U_2 + \frac{3}{4}\left\{\alpha_p\left[U_2^3 + U_1^2U_2(1+2\cos^2(\phi_d))\right] + \alpha_m\left[U_1^3 + 3U_1U_2^2\right]\cos(\phi_d) + 8\frac{\alpha_2}{m}U_2^3\right\} = 0. \tag{21b}$$

It can be seen from Eqs. (21) that the asymmetric configuration cannot exhibit single-mode solutions. Therefore, Eqs. (20) may both be simplified to

$$\left[2\alpha_p U_1 U_2 \cos(\phi_1-\phi_2) + \alpha_m\left(U_2^2+U_1^2\right)\right]\sin(\phi_1-\phi_2) = 0, \tag{22}$$

where $\phi_d = \phi_1 - \phi_2$ has been used. One solution to Eq. (22) involves setting the contents of the square brackets is zero; however, it is found that this is not possible for the case where the springs are hardening – this case is considered in [20], where softening behaviour is permitted. Therefore, Eq. (22) may only be satisfied by $\sin(\phi_1-\phi_2) = 0$.

Similar to the symmetric configuration, the condition $\sin(\phi_1-\phi_2) = 0$ leads to the phase relationship $\phi_1-\phi_2 = 0, \pi$, i.e. the modes may either be in-phase or in anti-phase. This allows the variable p to be defined as

$$p = \cos(\phi_1-\phi_2) = \begin{cases} +1 & \text{when } \phi_1-\phi_2 = 0, \\ -1 & \text{when } \phi_1-\phi_2 = \pi. \end{cases} \tag{23}$$

Note that the phase condition, defined by p, takes a different form in this example. Substituting this into Eqs. (21) gives the frequency–amplitude relationships

$$(\omega_{n1}^2-\omega^2)U_1 + \frac{3}{8m}\left[\alpha_1(U_1+pU_2)^3 + \alpha_3(U_1-pU_2)^3\right] = 0, \tag{24a}$$

$$(\omega_{n2}^2-\omega^2)U_2 + \frac{3}{8m}\left[\alpha_1(pU_1+U_2)^3 - \alpha_3(pU_1-U_2)^3 + 16\alpha_2U_2^3\right] = 0, \tag{24b}$$

where Eq. (8) has been used. Eqs. (24) may now be rearranged to give the frequency–amplitude relationships

$$\left[\frac{p3(\alpha_3-\alpha_1)}{8m}U_1^{-1}\right]U_2^4 + \left[\frac{3(8\alpha_2-\alpha_1-\alpha_3)}{4m}\right]U_2^3 + \left[\omega_{n2}^2-\omega_{n1}^2+\frac{3(\alpha_1+\alpha_3)}{4m}U_1^2\right]U_2 + \left[\frac{p3(\alpha_1-\alpha_3)}{8m}U_1^3\right] = 0, \tag{25a}$$

$$\omega^2 = \omega_{n1}^2 + \frac{3}{8m}\left[\alpha_1(U_1+pU_2)^3 + \alpha_3(U_1-pU_2)^3\right]U_1^{-1}, \tag{25b}$$

which may be solved to find the backbone curves of this system.

Fig. 3 shows the backbone curves of the 2-DOF oscillator for four different values of α_3, where $\alpha_1 \neq \alpha_3$ such that the system is asymmetric, and these are compared to the backbone curves of the symmetric configuration. It can be seen that, as a result of breaking the symmetry, the bifurcation on S_2 also breaks and forms an *imperfect bifurcation*. As a result of this imperfect bifurcation, an *isolated* backbone curve is formed, denoted $S_{1,2}^{i+}$ in Fig. 3a$_1$ and a$_2$, and $S_{1,2}^{i-}$ in Fig. 3b$_1$ and b$_2$. These are distinct from primary and secondary backbone curves, and cannot be traced to the zero-amplitude, trivial solution. As such, finding such backbone curves using techniques that rely upon an initial solution, such as numerical continuation, can prove challenging. Note that the superscripts $^{i+}$ and $^{i-}$ are used to denote isolated backbone curves where the modes are in- and out-of-phase, i.e. $p = +1$ and $p = -1$, respectively.

Recalling that, in the symmetric case, $\alpha_3 = 0.5$, Fig. 3 demonstrates that the *direction* in which the symmetry is broken dictates the direction in which the separation occurs in the bifurcated backbone curve. This can be seen in Fig. 3a$_1$ and a$_2$, representing breaking in the direction $\alpha_3 < \alpha_1$, and where the isolated backbone curve appears *below* the primary backbone

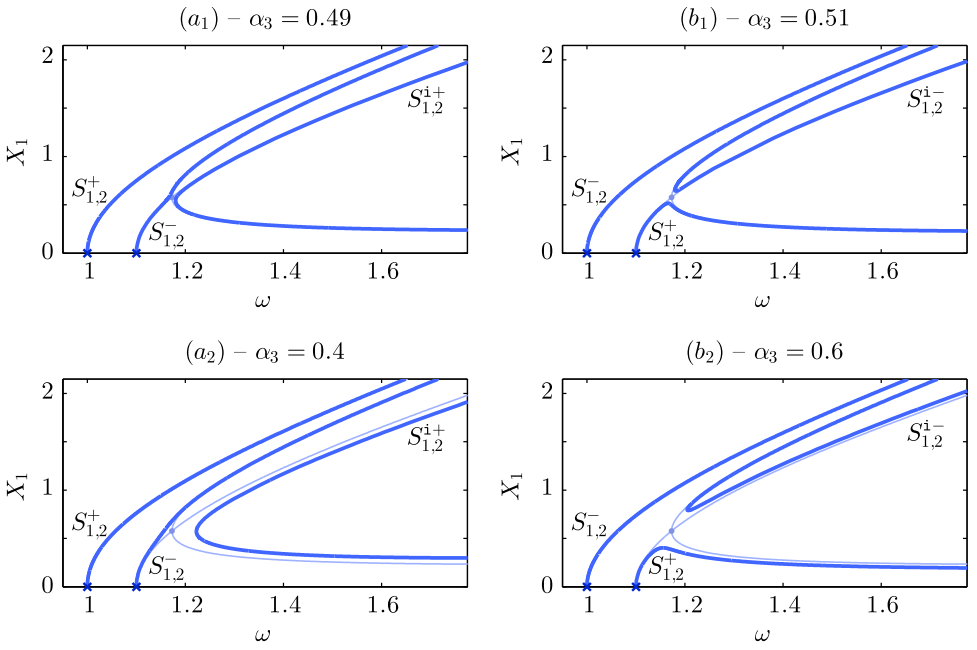

Fig. 3. The backbone curves of four different configurations of the example system, compared to those of the symmetric case. In all panels, dark-blue lines represent the asymmetric backbone curves, whilst light-blue lines show the symmetric backbone curves. Dark-blue crosses and light-blue dots mark the linear natural frequencies and the backbone curve bifurcations respectively. In all cases, the parameters are listed in Table 1, aside from α_3 which adopts a number of different values (as noted above each panel). All four panels are in the projection of the common response frequency, ω, against the displacement amplitude of the first mass, X_1. (For interpretation of the references to colour in this figure caption, the reader is referred to the web version of this paper.)

curves in this projection. Conversely, when the symmetry is broken such that $\alpha_3 > \alpha_1$, as shown in Fig. 3b$_1$ and b$_2$, the isolated backbone appears *above* the primary curve. As the high-amplitude response is often of primary concern in engineering, this appears to demonstrate that breaking the symmetry such that $\alpha_3 < \alpha_1$ is typically of lower concern in this system. However, it is worth noting that in the projection of ω against X_2, rather than against X_1, as shown in Fig. 3, this breaking appears to be reversed such that $\alpha_3 < \alpha_1$ leads to a higher-amplitude isolated backbone.

Recalling the schematic of the two-mass oscillator, Fig. 1, it can be seen that the symmetry of the unforced, undamped system may also be broken by changing the linear stiffness components – i.e. if the stiffness of the first grounding spring does not equal that of the second. It is found that this symmetry-breaking also results in a similar phenomenon, and isolated backbone curves are also formed. However, for the sake of brevity, this is not demonstrated here.

3. Determining the forced responses from the backbone curves

Whilst backbone curves provide valuable insight into the underlying dynamic behaviour of a system, they cannot be used directly to determine the forced responses. As forced responses are, ultimately, of greatest interest in many engineering applications, the ability to determine a direct link between the backbone curves and the forced responses provides numerous benefits. One method for achieving this is *energy transfer analysis*, detailed in [17]. An overview of this approach is now provided, and it is shown how it may be used to understand the forced responses of the example system using the backbone curves.

Energy transfer analysis relies on the observation that, for any steady-state response, the net energy transfer into a system, over one period of motion, must be zero – referred to as the *energy criterion*. The analysis also relies on the assumption that the forced responses at resonance share a solution with a backbone curve. From this it can be seen that, if a point on a backbone curve represents a solution for the forced response, it must satisfy the energy criterion. As such, it may also be assumed that any point on the backbone curve that does satisfy the energy criterion represents a solution to a resonant forced response, known as a *resonant crossing point*. For detailed discussion of the significance and validity of these assumptions, see [17].

In order to compute the energy transfer into and out-of the system, the nonconservative terms must be identified – i.e. the external forcing and damping terms. If $f_{i,k}$ represents the kth nonconservative term in the ith modal equation of motion,

the energy transfer into that mode over one period, as a result of that term, may be written as

$$E_{i,k} = \int_0^T f_{i,k}(t)\dot{q}_i(t)\mathrm{d}t, \tag{26}$$

where T is the period of the response of the system.

For the system considered here, the harmonics are assumed to be negligible, and hence the approximation $q_i = u_i$ is used. Using this, the nonconservative terms are found from Eqs. (6) and (7) as

$$f_{i,1} = 2\zeta\omega_{ni}\dot{u}_i, \tag{27a}$$

$$f_{i,2} = -P_{qi}\cos(\Omega t), \tag{27b}$$

where it has been recalled that $\mathbf{P}_u = \mathbf{P}_q$. Substituting these terms into Eq. (26), and using the assumed solution for u_i from Eq. (5), the external energy transfer may be written as

$$E_{i,1} = 2\zeta\omega_{ni}\omega^2 U_i^2 \int_0^T \left[\cos\left(\omega t - \phi_i - \frac{\pi}{2}\right)\right]^2 \mathrm{d}t, \tag{28a}$$

$$E_{i,2} = P_{qi}U_i\omega \int_0^T \cos(\Omega t)\cos\left(\omega t - \phi_i - \frac{\pi}{2}\right)\mathrm{d}t. \tag{28b}$$

Using $\Omega = \omega$, and calculating the period to be $T = 2\pi/\omega$, Eqs. (28) may be computed as

$$E_{i,1} = 2\pi\zeta\omega_{ni}\omega U_i^2, \tag{29a}$$

$$E_{i,2} = -\pi P_{qi}U_i \sin(\phi_i). \tag{29b}$$

As previously discussed, the energy criterion states that the total energy into the system over one period must be zero for any steady-state response. Therefore, if the ith modal equation of motion contains K_i nonconservative terms, this may be expressed as

$$\sum_{i=1}^{2}\sum_{k=1}^{K_i} E_{i,k} = 0, \tag{30}$$

which, substituting Eqs. (29), is written for the example system as

$$2\zeta\omega\left(\omega_{n1}U_1^2 + \omega_{n2}U_2^2\right) = P_{q1}U_1\sin(\phi_1) + P_{q2}U_2\sin(\phi_2). \tag{31}$$

Eq. (31) represents the energy relationship that must be satisfied in order for a backbone curve solution to represent a resonant crossing point. Note, however, that this expression contains the phase values ϕ_1 and ϕ_2. Whilst, for each backbone curve, the relationship between these values is known, the individual values are not known. As discussed in [17], these phase values may be found by considering that, in order for the forced response to cross a backbone curve precisely, the conservative components of the equation of motion must equate to zero independent of the nonconservative components. This may be expressed, for the ith mode, as

$$\sum_{k=1}^{K_i} f_{i,k} = 0, \tag{32}$$

which, using Eqs. (27), leads to

$$2\zeta\omega_{ni}U_i\omega\left[\cos\left(\phi_i + \frac{\pi}{2}\right) + \tan(\omega t)\sin\left(\phi_i + \frac{\pi}{2}\right)\right] + P_{qi} = 0. \tag{33}$$

From this it can be seen that $\sin(\phi_i + \frac{\pi}{2}) = 0$ is required for the expression to be time-invariant. As such, it is also required that $\cos(\phi_i + \frac{\pi}{2})$ is opposite in sign to P_{qi}, and therefore the phase of the ith mode is given by

$$\phi_i = \mathrm{sign}\{P_{qi}\}\frac{\pi}{2}. \tag{34}$$

The condition described by Eq. (32) is only satisfied under specific conditions, and hence, when these conditions are not satisfied, Eq. (34) is approximate. Now, substituting Eq. (34) into Eq. (31) gives

$$2\zeta\omega\left(\omega_{n1}U_1^2 + \omega_{n2}U_2^2\right) = P_{q1}U_1 + P_{q2}U_2. \tag{35}$$

The backbone curve solutions may now be substituted into Eq. (35) for specific forcing and damping values. It can be determined that any solution satisfying this expression must represent an approximate resonant crossing point. Note that this crossing point is precise if the phase relationship given by Eq. (34) is satisfied.

4. Isolas in the symmetric configuration

It has previously been observed that, for the symmetric configuration of the example system, no isolated backbone curves exist. We now investigate whether isolated forced responses, or *isolas*, may exist for this configuration.

When equal forcing is applied to both masses, i.e. $P_1 = P_2$, then, from Eqs. (4), it can be seen that the second linear mode is not directly forced, i.e. $P_{q2} = 0$. In this case, Eq. (35) may be written as

$$P_{q1} = 2\zeta\omega\frac{\omega_{n1}U_1^2 + \omega_{n2}U_2^2}{U_1}, \tag{36}$$

which may be used to determine the modal forcing amplitude required to cross a backbone curve at a given point. For the backbone curve S_2, described by Eq. (14b), $U_1 = 0$ throughout. From Eq. (36) it can be seen that no valid solution exists when $U_1 = 0$, therefore the forced response cannot cross S_2 at resonance for this forcing case. To determine the modal forcing amplitude required to cross the backbone curves S_1 and $S_{1,2}^{\pm}$, their solutions, given by Eqs. (14a) and (18), are substituted into Eq. (36).

The relationship between the first modal forcing amplitude, P_{q1}, and the locations of the resonant crossing points on the backbone curves S_1 and $S_{1,2}^{\pm}$ are shown in Fig. 4. This reveals that, even for very low excitation amplitudes, the forced response will cross S_1, whilst the $S_{1,2}^{\pm}$ backbone curves will not be crossed unless $P_{q1>0.0234}$. The specific case where $P_{q1} = 0.025$ is shown in Fig. 4 and the corresponding crossing points are highlighted. At this forcing amplitude, it can be seen that the forced response must cross the backbone curve at resonance at five points: once on S_1, twice on $S_{1,2}^{+}$ and twice on $S_{1,2}^{-}$. Note that $S_{1,2}^{+}$ and $S_{1,2}^{-}$ are superposed, and hence the predicted points shown in Fig. 4 represent resonant crossing points on both backbone curves. However, it cannot be directly determined whether these points correspond to an isola, as the points may all be connected via a continuous forced response curve, or via bifurcated forced response curves. In order to determine the nature of the forced responses, the branches must be computed.

It can be seen that Eq. (36) approaches an asymptote as $U_1 \to 0$ when $U_2 \neq 0$. Such a condition is met as the mixed-mode backbone curves, $S_{1,2}^{\pm}$, approach the bifurcation from S_2, and therefore corresponds to a vertical asymptote on the left-hand side of the $S_{1,2}^{\pm}$ curves in Fig. 4. This asymptotic behaviour may be understood physically by observing that the forcing is applied only to the first mode, and hence the energy input to the system, due to the forcing, will decrease as the first modal amplitude decreases. As a result, the forcing amplitude must increase in order to maintain the response in the second mode. If, instead, the forcing were applied to the second mode, i.e. if $P_{q2} \neq 0$, then such an asymptote would not exist, and a crossing at the bifurcation point may be achieved.

Fig. 5 shows the forced response branches of the symmetric configuration when forcing is applied at amplitude $[P_{q1},\ P_{q2}] = [0.025,\ 0]$. These are compared to the backbone curves of this configuration, along with the predicted resonant crossing points. Whilst the backbone curves have been computed using the second-order normal form technique, as described in Section 2, the forced branches have been computed using the numerical continuation software AUTO-07p [4]. The good agreement between the backbone curves and forced responses validates the assumptions used to find these backbone curves. It can be seen, however, that there is some disparity between S_1 and the forced response branch that envelops it, suggesting that the assumptions are less valid in this region. This may be due to the assumption that the harmonics are negligible, as the continuation data includes the harmonics. It may also be due to the assumptions that are inherent to the second-order normal form technique, which typically lose validity at higher amplitudes. If greater accuracy were required, the harmonics may be included, and the second-order normal form technique may be computed to a higher order of accuracy – see [13,24] for examples of this.

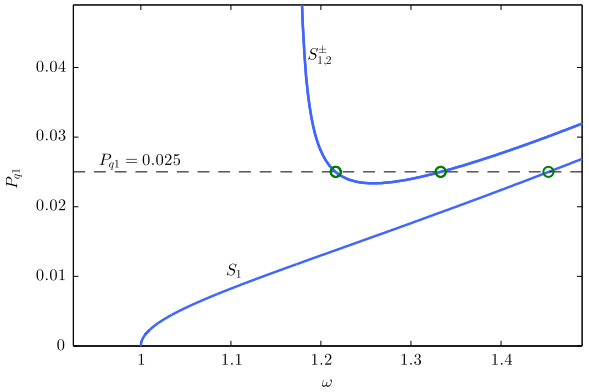

Fig. 4. The relationship between the first modal forcing amplitude, P_{q1}, and the positions of the resonant crossing points on the backbone curves for the symmetric configuration, with $P_{q2=0}$. This is shown in the projection of the common response frequency, ω, against the first modal forcing amplitude, P_{q1}. The loci of required forcing amplitudes, for each backbone curve, are represented by solid-blue lines. The specific case where the forcing amplitude is $P_{q1=0.025}$ is shown by a dashed-black line and the corresponding crossing points are highlighted by green circles. (For interpretation of the references to colour in this figure caption, the reader is referred to the web version of this paper.)

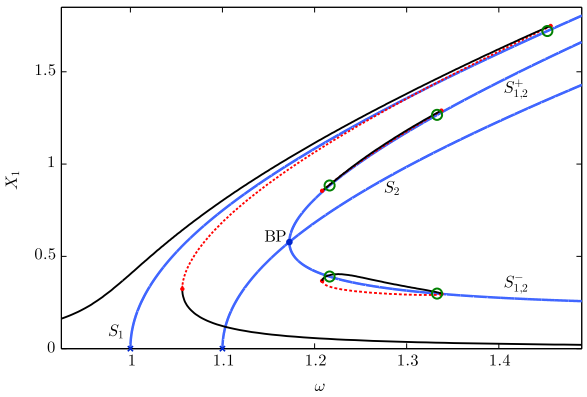

Fig. 5. The backbone and forced response curves for the symmetric configuration, with the forcing $P_{q1} = 0.025$. The backbone curves are represented by solid-blue lines, whilst solid-black and dashed-red lines represent the stable and unstable forced responses respectively. Dark-blue crosses mark the linear natural frequencies and a dark-blue dot, labelled "BP", represents the backbone curve bifurcation. Small-red dots show the fold bifurcations on the forced response curves. The green circles represent the predicted resonant crossing points, as given in Fig. 4. This figure is shown in the projection of the common response frequency, ω, against the displacement amplitude of the first mass, X_1. (For interpretation of the references to colour in this figure caption, the reader is referred to the web version of this paper.)

To generate these forced responses, the *primary* branch, enveloping S_1, was first computed. Comparing only the primary branch to the backbone curves and resonant crossing points, it is clear that not all crossing points have been reached, suggesting that additional responses exist. If numerical continuation is employed, the initial orbits may be generated using the amplitude, frequency and phase information provided by the second-order normal form technique at the crossing points. If these initial orbits are not sufficiently accurate, the resonant crossing points still indicate the existence of additional solution branches, and may be found using alternative techniques; for example, the continuation of fold bifurcations may be used to find the isolated solutions, see [9].

It is worth noting that the resonant crossing points only detect the crossing points between the forced response branches and backbone curves *at resonance*. Other crossing points that are observed are a feature of the projection used to represent the response. For example, in Fig. 5, the primary forced branch is seen to cross S_2 near to the second linear natural frequency; however, as this point is not resonant, it is not predicted as a crossing point. Furthermore, if this were to be viewed in a different projection, ω against X_2 for example, this apparent crossing point would occur at a different point.

It can also be seen in Fig. 5 that, whilst the resonant crossing points provide a good level of agreement between the predicted and true resonant points, they are not exact. This is due, in part, to the assumption that the forced responses cross the backbone curves precisely, which is only true under very specific conditions. This can be seen by considering the points on $S^{\pm}_{1,2}$, where both modes are active (and thus are both losing energy through damping) but only the first mode is forced. It is therefore clear that there must be a net energy transfer from the first mode into the second. However, any response that exhibits a net energy transfer between the modes cannot lie on a backbone curve, as backbone curves represent conservative responses. This observation underpins the method presented in [17], which allows the relative accuracy of the resonant crossing points to be estimated. This method also relies on the observation that energy transfer between the modes is only possible when there is a phase difference between the modes. As such, the phase difference that is required to support the necessary energy transfer may be computed, and used as a measure of the accuracy of the points – a predicted phase difference that is close to that of the backbone curve may be assumed to be accurate, whilst a large discrepancy suggests an inaccurate resonant crossing point. The details of how this phase is calculated are provided in [17].

Due to the symmetry of the system considered here, the estimated phase difference for the resonant crossing points on $S^+_{1,2}$ is the same as the corresponding points on $S^-_{1,2}$. For the lower points, near $\omega = 1.2$, the error in the phase difference is $\phi_1 - \phi_2 \approx 0.0995\pi$, whilst the higher points, near $\omega = 1.33$, predict an error of $\phi_1 - \phi_2 \approx 0.0267\pi$. Note that these are not intended to represent accurate predictions of the phase difference at resonance, but rather to provide a metric for estimating the accuracy of these points. As these errors are both relatively small, these points can be expected to be relatively accurate. Furthermore, as the difference is larger for the lower points than for the higher, it can be expected that the higher points are more accurate. These predictions are both confirmed in Fig. 5. This demonstrates the physical mechanism that governs the difference between the predicted resonant crossing points and the true resonant points. The method can also prove useful in assessing the relative accuracy of the points when the true responses are unknown, and for assessing the suitability of a resonant crossing point as an initial condition for numerical continuation. For the remainder of this paper, however, these metrics are not computed, as the forced responses are provided for comparison.

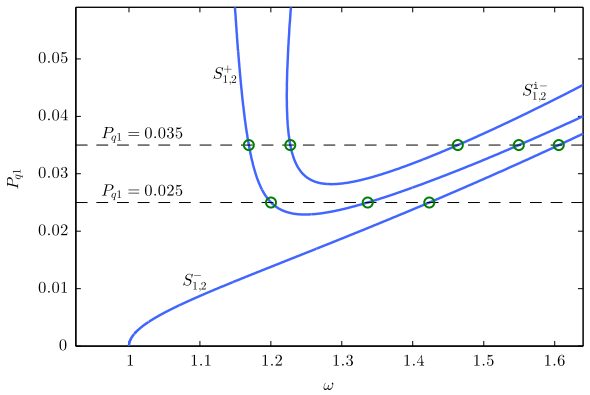

Fig. 6. The relationship between the first modal forcing amplitude, P_{q1}, and the positions of the resonant crossing points on the backbone curves for the asymmetric configuration. This is shown in the projection of the common response frequency, ω, against the first modal forcing amplitude, P_{q1}. The loci of required forcing amplitudes, for each backbone curve, are represented by solid-blue lines. The specific cases where the forcing amplitude is $P_{q1} = 0.025$ and $P_{q1} = 0.035$ are shown by dashed-black lines and the corresponding crossing points are highlighted by green circles. (For interpretation of the references to colour in this figure caption, the reader is referred to the web version of this paper.)

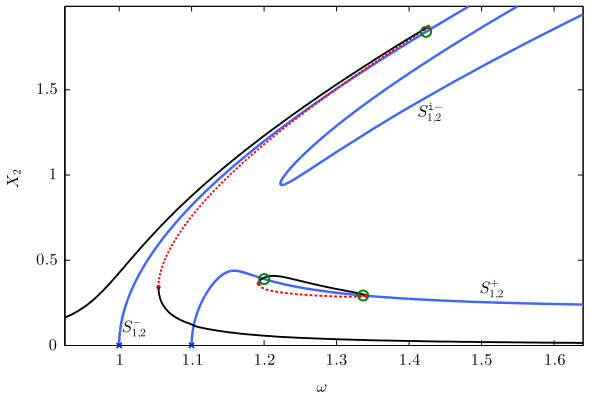

Fig. 7. The backbone and forced response curves for the asymmetric configuration, with the forcing $P_{q1} = 0.025$. The backbone curves are represented by solid-blue lines, whilst solid-black and dashed-red lines represent the stable and unstable forced responses respectively. Dark-blue crosses mark the linear natural frequencies and small-red dots show the fold bifurcations on the forced response curves. The green circles represent the predicted resonant crossing points, as given in Fig. 6. This figure is shown in the projection of the common response frequency, ω, against the displacement amplitude of the second mass, X_2. (For interpretation of the references to colour in this figure caption, the reader is referred to the web version of this paper.)

5. Isolas in the asymmetric configuration

In the previous section it was demonstrated that isolas may exist on the secondary backbone curves of the symmetric configuration, i.e. on $S^{\pm}_{1,2}$. In this section, the asymmetric configuration is considered for the case where $\alpha_3 = 0.4$, and the presence of isolas on primary and isolated backbone curves is investigated.

5.1. Single-mode forcing

As with the symmetric configuration, forcing in only the first linear mode is considered, allowing Eq. (36) to be used, together with Eqs. (25), to find the relationship between the forcing amplitude, P_{q1}, and the positions of the resonant crossing points. This relationship is shown in Fig. 6, and the specific cases where $P_{q1} = 0.025$ and $P_{q1} = 0.035$ are highlighted. From this it can be seen that, as with S_1 in the symmetric configuration, $S^{-}_{1,2}$ will be crossed at very low amplitudes. The primary backbone curve $S^{+}_{1,2}$ will not be crossed unless the forcing amplitude is sufficiently high, and the amplitude must be higher still in order for the isolated backbone curve $S^{i-}_{1,2}$ to be crossed. For the case where $P_{q1} = 0.025$, three crossing points are predicted: one on $S^{-}_{1,2}$ and two on $S^{+}_{1,2}$, suggesting that an isola *may* exist on $S^{+}_{1,2}$.

Fig. 7 shows the forced branches of the asymmetric configuration when forcing is applied at amplitude $[P_{q1}, P_{q2}] = [0.025, 0]$, along with the backbone curves and resonant crossing points for this case. As in the previous example, the forced responses have been computed using numerical continuation, and the good agreement between these responses and the backbone curves indicates a good level of accuracy in the computation of the backbone curves. The predicted resonant crossing points have again proved valuable in predicting the existence of an isola which, in this case,

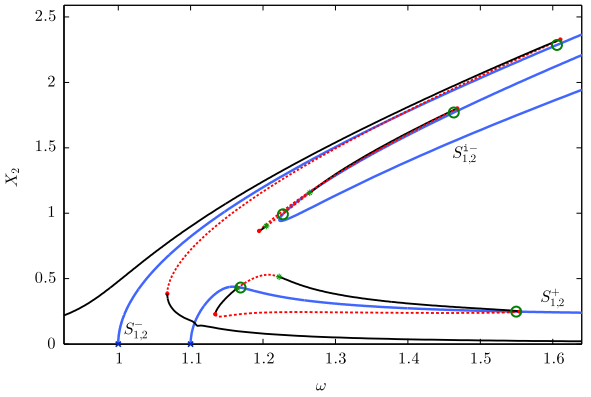

Fig. 8. The backbone and forced response curves for the asymmetric configuration, with the forcing $P_{q1} = 0.035$. The backbone curves are represented by solid-blue lines, whilst solid-black and dashed-red lines represent the stable and unstable forced responses respectively. Dark-blue crosses mark the linear natural frequencies. Small-red dots and green asterisks show the fold and torus bifurcations on the forced response curves respectively. The green circles represent the predicted resonant crossing points, as given in Fig. 6. This figure is shown in the projection of the common response frequency, ω, against the displacement amplitude of the second mass, X_2. (For interpretation of the references to colour in this figure caption, the reader is referred to the web version of this paper.)

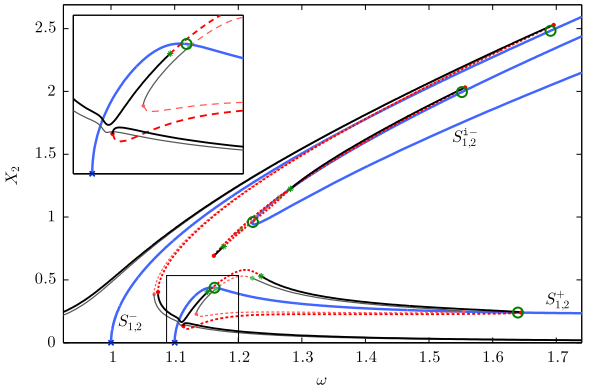

Fig. 9. The backbone and forced response curves for the asymmetric configuration, with the forcing $P_{q1} = 0.040$, showing a merging of an isola with the primary forced branch. The backbone curves are represented by solid-blue lines, whilst solid-black and dashed-red lines represent the stable and unstable forced responses respectively. Dark-blue crosses, small-red dots and green asterisks mark the linear natural frequencies, fold bifurcations and torus bifurcations respectively. The green circles represent the predicted resonant crossing points. The case where $P_{q1} = 0.035$, as shown in Fig. 8, is represented by thin, light lines. This figure is shown in the projection of the common response frequency, ω, against the displacement amplitude of the second mass, X_2. (For interpretation of the references to colour in this figure caption, the reader is referred to the web version of this paper.)

envelops a primary backbone curve. Without these crossing points, and noting the negligible influence of $S^{+}_{1,2}$ on the primary forced response branch, the presence of the isola would be difficult to predict.

When forcing is applied at amplitudes $[P_{q1},\ P_{q2}] = [0.035,\ 0]$, it can be seen from Fig. 6 that five resonant crossing points are predicted: one on $S^{-}_{1,2}$, two on $S^{+}_{1,2}$ and two on the isolated backbone curve $S^{i-}_{1,2}$. Fig. 8 shows the forced response branches for this case, along with the backbone curves and predicted resonant crossing points. From this it can be seen that an isola envelops the primary backbone curve $S^{+}_{1,2}$, which may be viewed as an evolution of the isola seen in Fig. 7. Additionally, in Fig. 8 there is an isola enveloping the isolated backbone curve $S^{i-}_{1,2}$. It is interesting to note that the primary forced branch appears to be influenced, to a small degree, by $S^{+}_{1,2}$; however, this small response is not resonant, and hence is not predicted by the resonant crossing points.

It is found, if the forcing amplitude is increased further, that the isola enveloping $S^{+}_{1,2}$ will merge with the primary forced branch. This is demonstrated in Fig. 9 which shows the case where the forcing amplitudes are $[P_{q1},\ P_{q2}] = [0.040,\ 0]$. The previous case, shown in Fig. 8, where $[P_{q1},\ P_{q2}] = [0.035,\ 0]$ is represented by thin lines. A detailed region shows that the small increase in the forcing amplitude leads to a merging of the isola that envelops $S^{+}_{1,2}$ and the primary forced branch. The isola that envelops $S^{i-}_{1,2}$ is seen to change under the increased forcing amplitude; however it does not merge with the primary branch. For this forcing configuration (i.e. in only the first linear mode), this isola remains isolated at amplitudes as high as $[P_{q1},\ P_{q2}] = [4,\ 0]$, 100 times of that shown in Fig. 9. It can therefore be assumed that, if this isola does merge with the primary branch, it will only do so at amplitudes beyond the region of validity of the analytical methods used here. This highlights the care that must be taken when using continuation techniques to find isolas, as this indicates that in the projection of Ω against P_{q1}, $S^{i-}_{1,2}$ may not be connected to the primary branch. As such, the resonant crossing points prove

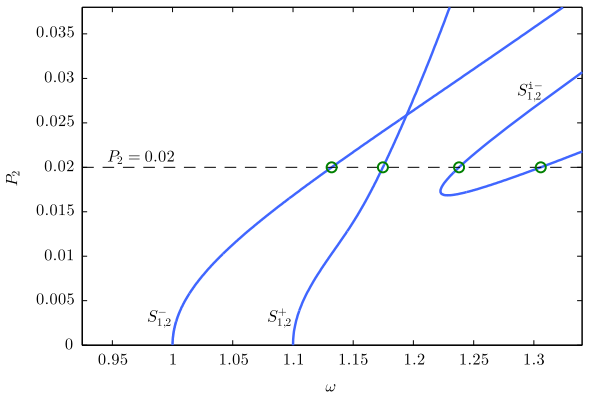

Fig. 10. The relationship between the amplitude of the forcing applied to the second mass, P_2, and the positions of the resonant crossing points on the backbone curves for the asymmetric configuration. This is shown in the projection of the common response frequency, ω, against the amplitude of the forcing at the second mass, P_2. The loci of required forcing amplitudes, for each backbone curve, are represented by solid-blue lines. The specific case where the forcing is at amplitude $[P_1,\ P_2] = [0,\ 0.02]$ is shown by a dashed-black line and the corresponding crossing points are highlighted by green circles. (For interpretation of the references to colour in this figure caption, the reader is referred to the web version of this paper.)

valuable for providing initial conditions for the continuation, or for informing the search using continuation in parameters other than Ω or P_{q1}.

5.2. Single-mass forcing

Previous examples in this paper have investigated the response of the two-mass oscillator to the single-mode forcing, requiring that both masses are forced with equal frequency and amplitude. Although such forcing is achievable for a two-mass oscillator, single-point excitation is more representative of real cases [18,25]. As such, the response of the system when forcing is applied to the second mass is now investigated.

From Eq. (4) it can be seen that forcing is applied to only the second mass when $P_{q1} = -P_{q2}$ and hence $P_2 = 2mP_{q1}$. Substituting this into Eq. (35) allows the relationship between the forcing amplitude, P_2, and the positions of the resonant crossing points to be found using

$$P_2 = \frac{4m\zeta\omega\left(\omega_{n1}U_1^2 + \omega_{n2}U_2^2\right)}{U_1 - U_2}. \tag{37}$$

The relationship described by Eq. (37) is shown in Fig. 10 using the backbone curves of the asymmetric configuration, and the case where the forcing is applied to the second mass at an amplitude of $P_2 = 0.02$ is highlighted. This case results in four resonant crossing points: one on each of the primary backbone curves, $S^{-}_{1,2}$ and $S^{+}_{1,2}$, and two on the isolated backbone curve, $S^{i-}_{1,2}$. This figure shows that $S^{+}_{1,2}$ will be crossed by the forced response when the forcing amplitude is very low. This is in contrast to the case where the forcing was applied in only the first mode, as shown in Fig. 6, where a sufficiently high forcing amplitude is required before this backbone curve is crossed.

The forced response branches and backbone curves for the asymmetric configuration, when forcing is applied to the second mass with an amplitude of $P_2 = 0.02$, are shown in Fig. 11. This demonstrates that an isola may exist in the forced response when forcing is applied to just one mass, and that this isola envelops the isolated backbone curve $S^{i-}_{1,2}$. It can be seen that, for this case, $S^{+}_{1,2}$ is crossed by a primary forced branch. This is in contrast to the cases where forcing is applied in only the first mode, shown in Figs. 7 and 8, where $S^{+}_{1,2}$ is crossed by an isola at resonance.

Furthermore, it may be assumed that, for an isola to envelop a single backbone curve, there must be at least two resonant crossing points on that backbone curve. It can be seen from Fig. 10 that, for the primary backbone curves $S^{+}_{1,2}$ and $S^{-}_{1,2}$, when the forcing is applied to just the second mass, the loci of resonant crossing point positions are monotonic, for the range of forcing amplitudes shown. As such, when forcing amplitude is fixed, only one crossing point will be seen on each of these backbone curves, and hence an isola cannot envelop these curves independently.

6. Conclusions

This paper has shown how isolated responses, in both the backbone curves and the forced responses, may exist in different configurations of a two-mass oscillator with cubic nonlinear springs. This was first demonstrated by showing how, by breaking the symmetry of the system, the bifurcations on the backbone curves can break to form imperfect bifurcations, resulting in isolated backbone curves. The second-order normal form technique was used to generate analytical descriptions of the backbone curves, and closed-form solutions were obtained, allowing the isolated backbone curves to be computed naturally. Whilst it may not be possible to obtain closed-form solutions for more complex systems, it has been shown that

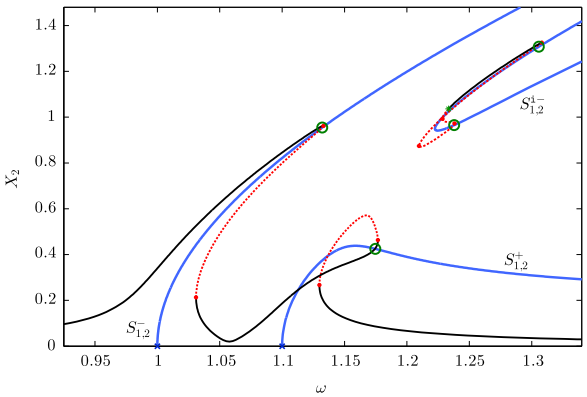

Fig. 11. The backbone and forced response curves for the asymmetric configuration, with forcing at amplitude $P_2 = 0.02$ applied to the second mass. The backbone curves are represented by solid-blue lines, whilst solid-black and dashed-red lines show the stable and unstable forced responses respectively. Dark-blue crosses mark the linear natural frequencies. Small-red dots and green asterisks show the fold and torus bifurcations on the forced response curves respectively. The green circles represent the predicted resonant crossing points, as given in Fig. 10. This figure is shown in the projection of the common response frequency, ω, against the displacement amplitude of the second mass, X_2. (For interpretation of the references to colour in this figure caption, the reader is referred to the web version of this paper.)

the backbone curves represent a simpler problem than the forced responses, due to the fixed phase relationships between the modes. As such, in complex systems, where finding isolas becomes impractical, the use of iterative techniques for finding isolated backbone curves may still be feasible.

The use of an energy-based technique to find the resonant crossing points of forced responses on backbone curves was then demonstrated. Although these points do not directly reveal the existence of isolas, they do indicate whether or not all forced responses have been computed. Additionally, the crossing points may be used to understand the nature of the isolas, thus simplifying the task of finding and computing the responses. The energy analysis was used to find the range of forcing amplitudes that lead to isolas in the symmetric configuration of the example system. Next, it was shown that an isola may envelop a primary backbone curve of the asymmetric configuration. When a higher forcing amplitude is applied, this isola becomes larger, and an additional isola forms around the isolated backbone curve. These cases reveal how the relationship between the forcing amplitude and the resonant crossing point locations, described by the energy analysis, may be used to give great insight into the nature of the forced responses. Finally, the case where forcing was applied to just one of the masses was considered. This represents a more typical case for such a system, and it was shown that an isola may also exist under such conditions.

Whilst the ability to compute isolated backbone curve in large systems still poses a significant challenge, many of the isolas shown in this paper envelop primary backbone curves. As these may be computed for relatively large and complex systems, using numerical continuation, the approach demonstrated in this paper may be extended to such systems.

Acknowledgements

The authors would like to acknowledge the support of the Engineering and Physical Sciences Research Council. T.L.H. and S.A.N. are supported by EP/K005375/1. The data presented in this work are openly available from the University of Bristol repository at http://dx.doi.org/10.5523/bris.1nrlxw9m27k7g1s5pyuxomgs46.

References

[1] A.H. Nayfeh, D.T. Mook, *Nonlinear Oscillations, Physics Textbook*, Wiley, Weinheim, Germany, 1995.
[2] P. Glendinning, *Stability, Instability and Chaos: An Introduction to the Theory of Nonlinear Differential Equations, Cambridge Texts in Applied Mathematics*, Cambridge University Press, Cambridge, UK, 1994.
[3] L. Jezequel, C.H. Lamarque, Analysis of non-linear dynamical systems by the normal form theory, *Journal of Sound and Vibration* 149 (3) (1991) 429–459, http://dx.doi.org/10.1016/0022-460X(91)90446-Q.
[4] E.J. Doedel, with major contributions from A.R. Champneys, T.F. Fairgrieve, Y.A. Kuznetsov, F. Dercole, B.E. Oldeman, R.C. Paffenroth, B. Sandstede, X.J. Wang, C. Zhang, *AUTO-07P: Continuation and Bifurcation Software for Ordinary Differential Equations*, Concordia University, Montreal, Canada, Available at: ⟨http://cmvl.cs.concordia.ca/⟩, 2008.
[5] H. Dankowicz, F. Schilder, *Recipes for Continuation*, Society for Industrial and Applied Mathematics, Philadelphia, PA, 2013. http://dx.doi.org/10.1137/1.9781611972573.
[6] M. Peeters, R. Viguié, G. Sérandour, G. Kerschen, J.-C. Golinval, Nonlinear normal modes, Part II: *toward a practical computation using numerical continuation techniques*, *Mechanical Systems and Signal Processing* 23 (1) (2009) 195–216, http://dx.doi.org/10.1016/j.ymssp.2008.04.003. Special Issue: Non-linear Structural Dynamics.
[7] G. Von Groll, D.J. Ewins, The harmonic balance method with arc-length continuation in rotor/stator contact problems, *Journal of Sound and Vibration* 241 (2) (2001) 223–233.

[8] T. Detroux, L. Renson, L. Masset, G. Kerschen, The harmonic balance method for bifurcation analysis of large-scale nonlinear mechanical systems, *Computer Methods in Applied Mechanics and Engineering* 296 (2015) 18–38, http://dx.doi.org/10.1016/j.cma.2015.07.017.
[9] R.J. Kuether, L. Renson, T. Detroux, C. Grappasonni, G. Kerschen, M.S. Allen, Nonlinear normal modes, modal interactions and isolated resonance curves, *Journal of Sound and Vibration* 351 (2015) 299–310, http://dx.doi.org/10.1016/j.jsv.2015.04.035.
[10] J.-P. Noël, T. Detroux, L. Masset, G. Kerschen, L. Virgin, Isolated response curves in a base-excited, two-degree-of-freedom, nonlinear system, *ASME 2015 International Design Engineering Technical Conferences and Computers and Information in Engineering Conference, American Society of Mechanical Engineers*, 2015. http://dx.doi.org/10.1115/DETC2015-46106.
[11] N.A. Alexander, F. Schilder, Exploring the performance of a nonlinear tuned mass damper, *Journal of Sound and Vibration* 319 (1–2) (2009) 445–462, http://dx.doi.org/10.1016/j.jsv.2008.05.018.
[12] T.L. Hill, A. Cammarano, S.A. Neild, D.J. Wagg, Out-of-unison resonance in weakly nonlinear coupled oscillators, *Proceedings of the Royal Society of London A: Mathematical, Physical and Engineering Sciences* 471 (2014) 2173. http://dx.doi.org/10.1098/rspa.2014.0659.
[13] S.A. Neild, D.J. Wagg, Applying the method of normal forms to second-order nonlinear vibration problems, *Proceedings of the Royal Society A: Mathematical, Physical and Engineering Science* 467 (2011) 1141–1163. http://dx.doi.org/10.1098/rspa.2010.0270.
[14] A. Cammarano, T.L. Hill, S.A. Neild, D.J. Wagg, Bifurcations of backbone curves for systems of coupled nonlinear two mass oscillator, *Nonlinear Dynamics* 77 (1–2) (2014) 311–320, http://dx.doi.org/10.1007/s11071-014-1295-3.
[15] K. Ikeda, K. Murota, *Imperfect Bifurcation in Structures and Materials: Engineering Use of Group-Theoretic Bifurcation Theory, Applied Mathematical Sciences*, Springer, New York, 2002.
[16] T. Hill, A. Cammarano, S. Neild, D. Wagg, An analytical method for the optimisation of weakly nonlinear systems, *Proceedings of EURODYN 2014*, 2014, pp. 1981–1988.
[17] T.L. Hill, A. Cammarano, S.A. Neild, D.J. Wagg, Interpreting the forced responses of a two-degree-of-freedom nonlinear oscillator using backbone curves, *Journal of Sound and Vibration* 349 (2015) 276–288, http://dx.doi.org/10.1016/j.jsv.2015.03.030.
[18] A.D. Shaw, T.L. Hill, S.A. Neild, M.I. Friswell, Periodic responses of a structure with 3:1 internal resonance, *Mechanical Systems and Signal Processing* (2016), in press. http://dx.doi.org/10.1016/j.ymssp.2016.03.008.
[19] T. Detroux, J.P. Noël, G. Kerschen, L.N. Virgin, Experimental study of isolated response curves in a two-degree-of-freedom nonlinear system, *Proceedings of the International Modal Analysis Conference*, 2016.
[20] T.L. Hill, Modal Interactions in Nonlinear Systems, PhD Thesis, University of Bristol, 2016. http://dx.doi.org/10.13140/rg.2.1.2720.9368.
[21] T.L. Hill, P.L. Green, A. Cammarano, S.A. Neild, Fast Bayesian identification of a class of elastic weakly nonlinear systems using backbone curves, *Journal of Sound and Vibration* 360 (2015) 156–170, http://dx.doi.org/10.1016/j.jsv.2015.09.007.
[22] D.J. Wagg, S.A. Neild, Approximate methods for analysing nonlinear vibrations, *Nonlinear Vibration with Control, Solid Mechanics and Its Applications*, Vol. 218, Springer International Publishing, Dordrecht, The Netherlands, 2015, pp. 145–209. http://dx.doi.org/10.1007/978-3-319-10644-1_4.
[23] S.A. Neild, D.J. Wagg, A generalized frequency detuning method for multidegree-of-freedom oscillators with nonlinear stiffness, *Nonlinear Dynamics* 73 (1–2) (2013) 649–663, http://dx.doi.org/10.1007/s11071-013-0818-7.
[24] S.A. Neild, A.R. Champneys, D.J. Wagg, T.L. Hill, A. Cammarano, The use of normal forms for analysing nonlinear mechanical vibrations, *Philosophical Transactions of the Royal Society of London A: Mathematical, Physical and Engineering Sciences* 373 (2015) 2051, http://dx.doi.org/10.1098/rsta.2014.0404.
[25] A. Gonzalez-Buelga, S.A. Neild, D.J. Wagg, J.H.G. Macdonald, Modal stability of inclined cables subjected to vertical support excitation, *Journal of Sound and Vibration* 318 (3) (2008) 565–579, http://dx.doi.org/10.1016/j.jsv.2008.04.031.